

AD-A128 491

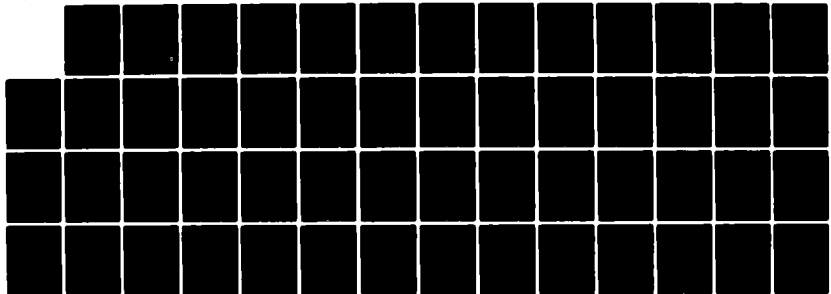
GRID GENERATION ABOUT A FIN-CYLINDER COMBINATION(U)
PENNSYLVANIA STATE UNIV UNIVERSITY PARK APPLIED
RESEARCH LAB G H HOFFMAN 30 MAR 83 ARL/PSU/TM-83-45
N00024-79-C-6043

1/1

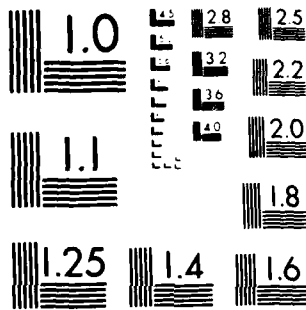
UNCLASSIFIED

F/G 12/1

NL



END
DATE
FILMED
6-83
DTIC



MICROCOPY RESOLUTION TEST CHART
NATIONAL BUREAU OF STANDARDS 1963-A

6

DA 1284

GRID GENERATION ABOUT A FIN-CYLINDER
COMBINATION

G. H. Hoffman

Technical Memorandum
File No. TM-83-45
30 March 1983
Contract No. N00024-79-C-6043

Copy No. 7

The Pennsylvania State University
Intercollege Research Programs and Facilities
APPLIED RESEARCH LABORATORY
Post Office Box 30
State College, PA 16801

Approved for Public Release
Distribution Unlimited

DTIC
ELECTE
MAY 24 1983
S E D

DTIC FILE COPY

83 05 23 063

UNCLASSIFIED

SECURITY CLASSIFICATION OF THIS PAGE (When Data Entered)

REPORT DOCUMENTATION PAGE		READ INSTRUCTIONS BEFORE COMPLETING FORM
1. REPORT NUMBER TM 83-45	2. GOVT ACCESSION NO. DA-112849	3. RECIPIENT'S CATALOG NUMBER
4. TITLE (and Subtitle) GRID GENERATION ABOUT A FIN-CYLINDER COMBINATION		5. TYPE OF REPORT & PERIOD COVERED Technical Memorandum
		6. PERFORMING ORG. REPORT NUMBER
7. AUTHOR(s) G. H. Hoffman		8. CONTRACT OR GRANT NUMBER(s) N00024-79-C-6043
9. PERFORMING ORGANIZATION NAME AND ADDRESS Applied Research Laboratory Post Office Box 30 State College, PA 16801		10. PROGRAM ELEMENT, PROJECT, TASK AREA & WORK UNIT NUMBERS
11. CONTROLLING OFFICE NAME AND ADDRESS Naval Sea Systems Command Code NSEA-63R31 Washington, DC 20362		12. REPORT DATE 30 March 1983
		13. NUMBER OF PAGES 56
14. MONITORING AGENCY NAME & ADDRESS (if different from Controlling Office)		15. SECURITY CLASS. (of this report)
		15a. DECLASSIFICATION/DOWNGRADING SCHEDULE
16. DISTRIBUTION STATEMENT (of this Report) Approved for public release. Distribution unlimited. Per NAVSEA -		
17. DISTRIBUTION STATEMENT (of the abstract entered in Block 20, if different from Report)		
18. SUPPLEMENTARY NOTES		
19. KEY WORDS (Continue on reverse side if necessary and identify by block number) three-dimensional, grid, generation, cylinder		
20. ABSTRACT (Continue on reverse side if necessary and identify by block number) An algebraic grid generation procedure is presented which produces a three-dimensional, body fitted coordinate system about a right circular cylinder with four symmetric fins attached. Special features of the grid are an initial value plane normal to the cylinder axis and the ability to cluster lines near the fin and cylinder surfaces for viscous/turbulent flow calculations. The method used is a modification of the		

DD FORM 1473
1 JAN 73

EDITION OF 1 NOV 65 IS OBSOLETE

UNCLASSIFIED

SECURITY CLASSIFICATION OF THIS PAGE (When Data Entered)

UNCLASSIFIED

SECURITY CLASSIFICATION OF THIS PAGE(When Data Entered)

Jameson-Caughey procedure developed originally for inviscid transonic flow calculations about wing-fuselage combinations. In this procedure, a sequence of conformal transformations followed by a shearing transformation is used to map the irregular flow domain in physical space into a rectangular shaped computational domain. A three-dimensional grid is produced by stacking two-dimensional mappings. The method is therefore extremely fast. The main features of the procedure are discussed and two numerical examples of grids are presented for a fin composed of a symmetric Joukowski airfoil.

UNCLASSIFIED

SECURITY CLASSIFICATION OF THIS PAGE(When Data Entered)



Accession For	
NTIS GRA&I	<input checked="" type="checkbox"/>
DTIC TAB	<input type="checkbox"/>
Unannounced	<input type="checkbox"/>
Justification	
By _____	
Distribution/ _____	
Availability Codes	
Aval and/or	
Dist	Special
A	

Subject: Grid Generation about a Fin-Cylinder Combination

References: See Page 29

Abstract: An algebraic grid generation procedure is presented which produces a three-dimensional, body fitted coordinate system about a right circular cylinder with four symmetric fins attached. Special features of the grid are an initial value plane normal to the cylinder axis and the ability to cluster lines near the fin and cylinder surfaces for viscous/turbulent flow calculations. The method used is a modification of the Jameson-Caughey procedure developed originally for inviscid transonic flow calculations about wing-fuselage combinations. In this procedure, a sequence of conformal transformations followed by a shearing transformation is used to map the irregular flow domain in physical space into a rectangular shaped computational domain. A three-dimensional grid is produced by stacking two-dimensional mappings. The method is therefore extremely fast. The main features of the procedure are discussed and two numerical examples of grids are presented for a fin composed of a symmetric Joukowski airfoil.

Acknowledgment: This work was sponsored by the Office of Naval Research under the Fundamental Research Initiatives Program.

TABLE OF CONTENTS

	<u>Page</u>
Abstract	1
Acknowledgment	1
List of Figures	3
List of Tables	4
I. Introduction	5
II. Analysis	6
2.1 Geometry of Computational Domain	6
2.2 Sequence of Transformations	7
2.3 Conformal Mapping Relations	10
2.4 Calculation of Shearing Boundaries	13
2.5 Stretching Functions	16
III. Results and Discussion	22
3.1 Generation of the Grid	22
3.2 Features of the Grid	24
3.3 Numerical Examples	27
References	29
Figures	30
Appendix: Grid Generation Computer Code Listing	43

LIST OF FIGURES

- Figure 1. Schematic of Geometry and Computational Domain.
- Figure 2. Coordinate System in Crossflow Plane.
- Figure 3. Computational Domain in $(\bar{x}, \bar{\theta})$ Plane.
- Figure 4. Boundary Images in (ξ, η) Plane.
- Figure 5. Boundary Images in $(\bar{\xi}, \bar{\eta})$ Plane.
- Figure 6. Schematic of Computational Plane.
- Figure 7. Two-Sided Stretching Function for Y.
- Figure 8. One-Sided Stretching Function for Z.
- Figure 9. Three Segment Stretching Function for X.
- Figure 10. Effect of Singularity Location on Upper Shearing Boundary.
- Figure 11. Ellipticity of Initial Value Line in (ξ, η) Plane.
- Figure 12. Grid for a Twelve Percent Thick Joukowsky Airfoil.
- Figure 13. Grid for a Six Percent Thick Joukowsky Airfoil.

LIST OF TABLES

Table 1. Grid Parameters for Numerical Examples.

I. INTRODUCTION

This report addresses the problem of generating a surface-fitted grid in a model fin-body problem consisting of a circular cylinder with four identical symmetric fins attached. This grid is to be used in the calculation of incompressible, laminar flow at moderate-to-high Reynolds numbers. The aim of the calculation is to resolve the details of the separated zone at the leading edge of the fin-cylinder juncture and the subsequent vortex that forms downstream. Thus, the grid must have proper clustering so as to resolve the regions of high flow gradients.

The approach used here is to generate the grid analytically but to determine the metric coefficients numerically. Such an approach has been pursued successfully by Jameson [1] and Caughey and Jameson [2-4] in solving three-dimensional inviscid transonic flows about wing-body combinations. The basic idea is to map the physical geometry to a strip of almost constant width using a sequence of conformal transformations. Then boundary fitted coordinates are generated by the application of a shearing transformation. The result of the latter transformation is a nonorthogonal coordinate system in the physical plane but one in which the nonorthogonality can be controlled.

The present work is an extension of the Jameson-Caughey technique for what is called the wind tunnel problem to the case of an initial value plane ahead of the airfoil. In order to treat viscous flow, clustering transformations are used so that the computational grid is uniform in all three directions.

One advantage of the present technique is that, owing to the simple cylindrical body geometry, a three-dimensional grid is generated by stacking a series of two-dimensional grids. Another advantage of the analytical approach over the numerical solution of elliptic partial differential equations as a

means of grid generation is its much greater speed which is especially important for three-dimensional applications.

II. ANALYSIS

2.1 Geometry of Computational Domain

We start the grid generation analysis by defining the geometry about which a surface fitted grid is to be generated and the extent of the computational domain.

1. The body is an infinitely long, hollow circular cylinder of radius R_c with its centerline parallel to the free-stream velocity vector.
2. Four identical fins of constant unit chord and infinite span, consisting of symmetric airfoil sections, are mounted on the cylinder 90 degrees apart with their chord planes passing through the cylinder axis.
3. The computational domain consists of the region interior to an outer cylinder of radius R_t which encases the inner cylinder and fins, bounded upstream and downstream by planes normal to the cylinder axis.

A schematic of one fourth of the geometry and computational domain is shown in Fig. 1 and a head-on view showing the coordinate system in the crossflow plane appears in Fig. 2. Since the fins are identical and equally spaced, we have four planes of symmetry, namely, at $\theta = 0, \pi/4, \pi/2$ and $3\pi/4$. Thus, in the flow field calculation for this model problem only the segment $0 < \theta < \pi/4$ needs to be considered.

2.2 Sequence of Transformations

Four transformations applied in sequence are required to map the fin-cylinder and surrounding computational domain into a rectangular parallelepiped. Then a fifth stretching transformation is applied to adjust the grid line spacings for proper flow field resolution in physical space and to allow a uniform step size in all three computational coordinates.

We start by defining polar coordinates (r, θ) in the crossflow plane, as shown in Fig. 2, according to

$$r = (y^2 + z^2)^{1/2} , \quad (1)$$

$$\theta = \tan^{-1} \left(\frac{y}{z} \right) . \quad (2)$$

Thus, points in physical space are defined by standard cylindrical coordinates (x, r, θ) .

Following Caughey and Jameson [2], the first transformation normalizes (x, r, θ) according to (all lengths are referred to the airfoil chord):

$$\bar{x} = x - d_s + \ln 2 , \quad (3)$$

$$\bar{r} = \frac{r - R_c}{R_t - R_c} , \quad (4)$$

$$\bar{\theta} = 4\theta , \quad (5)$$

where d_s is the location of the singular point of the unwrapping transformation and is just inside the leading edge of the airfoil. Note that in the above definitions, $0 < \bar{r} < 1$ and $0 < \bar{\theta} < \pi$ in the computational domain. The upper limit on $\bar{\theta}$ is convenient in the next transformation.

Because $\bar{r} = \text{constant}$ is a surface fitted coordinate we need only generate a surface fitted grid in the $(\bar{x}, \bar{\theta})$ plane. The geometry of an $\bar{r} = \text{constant}$ surface in the computational domain is sketched in Fig. 3.

The conformal transformation

$$\bar{x} - i\bar{\theta} = \ln[1 - \cosh(\xi + i\eta)] , \quad (6)$$

applied to an $\bar{r} = \text{constant}$ surface unwraps the geometry in Fig. 3 to produce the domain shown in Fig. 4. The minus sign has been used on the left in Eq. (6) so that the upper symmetry plane maps to the positive ξ axis.

In the present problem initial conditions from an axisymmetric boundary layer-potential flow composite solution are specified on the plane $\bar{x} = -\bar{a}$. This initial value line in an $\bar{r} = \text{constant}$ surface (IVL) is shown as line segment ABC in Fig. 3. Under transformation (6), the IVL maps to a near semi-circle in the (ξ, η) plane, as shown in Fig. 4. The airfoil image in this plane is the arc DEF.

We next apply another conformal transformation to nearly straighten out the IVL in Fig. 4. This transformation is

$$\bar{\xi} + i\bar{\eta} = \xi + i\eta + \frac{\xi_0^2}{\xi + i\eta} , \quad (7)$$

where ξ_0 is the intersection of the IVL with the ξ axis (Point A in Fig. 4). The conformal transformation (7) maps the upper and lower boundaries in the (ξ, η) plane into slowly varying functions of $\bar{\xi}$ in the $(\bar{\xi}, \bar{\eta})$ plane, as shown in Fig. 5. We note that near Points A and C the IVL is now cusp-like.

The fourth transformation is a shearing transformation which straightens out the upper and lower boundaries in the $(\bar{\xi}, \bar{\eta})$ plane. This transformation is

$$X = \bar{\xi} , \quad (8)$$

$$Y = \frac{\bar{\eta} - \bar{\eta}_L}{D} , \quad (9)$$

$$Z = \bar{r} , \quad (10)$$

where

$$D \equiv D(\bar{\xi}, \bar{r}) = \bar{\eta}_U - \bar{\eta}_L , \quad (11)$$

and $\bar{\eta}_U$ and $\bar{\eta}_L$ are the ordinates, at a given $\bar{\xi}$, of the upper and lower boundaries in the $(\bar{\xi}, \bar{\eta})$ plane.

Finally, to provide for clustering the grid lines near the fin and cylinder surfaces to resolve the viscous layers there and to space lines around the airfoil and in the wake as desired, we introduce one-dimensional stretching functions as follows:

$$X_c = F_1(X) , \quad (12)$$

$$Y_c = F_2(Y) , \quad (13)$$

$$Z_c = F_3(Z) , \quad (14)$$

For the time being we leave F_1 , F_2 and F_3 unspecified. Thus (X_c, Y_c, Z_c) are the computational coordinates devised so that the step sizes ΔX_c , ΔY_c and ΔZ_c are constants.

2.3 Conformal Mapping Relations

Since the FORTRAN code is written in terms of real variables, the real and imaginary parts of the conformal mappings must be determined. In addition, the inverses of both mappings are needed because the grid generation procedure requires being able to proceed from the $(\bar{x}, \bar{\theta})$ plane to the (X_c, Y_c) plane and then back to the $(\bar{x}, \bar{\theta})$ plane.

The real and imaginary parts of Eq. (6) yield the two relations:

$$\cosh \xi \cos \eta = 1 - e^{\bar{x}} \cos \bar{\theta} , \quad (15)$$

$$\sinh \xi \sin \eta = e^{\bar{x}} \sin \bar{\theta} . \quad (16)$$

The solutions for \bar{x} and $\bar{\theta}$ are obtained by squaring (15) and (16), then adding and making use of the ordinary and hyperbolic trigonometric identities. The result for \bar{x} , choosing the proper sign, is

$$\bar{x} = \ln(\cosh \xi - \cos \eta) , \quad (17)$$

and $\bar{\theta}$ is obtained from Eq. (15), viz.,

$$\bar{\theta} = \cos^{-1} \left(\frac{1 - \cosh \xi \cos \eta}{\cosh \xi - \cos \eta} \right) . \quad (18)$$

To obtain the solutions for ξ and η we first define,

$$\bar{p} = 1 - e^{\bar{x}} \cos \bar{\theta} , \quad (19)$$

$$\bar{q} = e^{\bar{x}} \sin \bar{\theta} . \quad (20)$$

Following the same procedures as above, we eliminate η to obtain a quadratic

equation for $\sinh^2 \xi$ which has the solution

$$\sinh^2 \xi = \frac{1}{2} [(\beta^2 + 4q^2)^{1/2} - \beta] \quad (21)$$

where

$$\beta = 1 - \frac{p^2}{q^2} - \frac{q^2}{p^2} . \quad (22)$$

In the right half plane ξ is the positive root of Eq. (21). The expression for η with the proper behavior ($0 < \eta < \pi$) is obtained from Eq. (15), viz.

$$\eta = \cos^{-1} \left[\frac{\bar{p}}{\cosh \xi} \right] . \quad (23)$$

Next, the real and imaginary parts of Eq. (7) yield

$$\bar{\xi} = \xi \left[1 + \frac{\xi_0^2}{\xi^2 + \eta^2} \right] , \quad (24)$$

$$\bar{\eta} = \eta \left[1 - \frac{\xi_0^2}{\xi^2 + \eta^2} \right] . \quad (25)$$

We determine ξ_0 from Eq. (17) by setting $\bar{x} = -\bar{a} = -a + \ln 2$ and $\eta = 0$. The result is

$$\xi_0 = \cosh^{-1}(1 + 2e^{-a}) . \quad (26)$$

where $a = d_s + d_{IVL}$.

To solve for ξ and η in terms $\bar{\xi}$ and $\bar{\eta}$ we return to the complex form which is written as,

$$w = z + \frac{\xi_0^2}{z} , \quad (27)$$

where

$$w = \bar{\xi} + i\bar{\eta} , \quad (28)$$

$$z = \xi + i\eta . \quad (29)$$

Solving Eq. (27) for z yields,

$$\phi^2 = \frac{1}{4} w^2 - \xi_0^2 , \quad (30)$$

where

$$\phi = z - \frac{1}{2} w . \quad (31)$$

Let us now define

$$\phi = u + iv . \quad (32)$$

Then, combining Eqs. (28), (29) and (31) gives:

$$\xi = u + \frac{1}{2} \bar{\xi} , \quad (33)$$

$$\eta = v + \frac{1}{2} \bar{\eta} . \quad (34)$$

Now Eq. (30) leads to the following relations:

$$u^2 - v^2 = \hat{p} , \quad (35)$$

$$uv = \hat{q} , \quad (36)$$

where

$$\hat{p} = \frac{1}{4} (\bar{\xi}^2 - \bar{\eta}^2) - \xi_0^2 , \quad (37)$$

$$\hat{q} = \frac{1}{4} \bar{\xi} \bar{\eta} . \quad (38)$$

Equations (35) and (36) can be solved for u and v with the result:

$$u^2 = \frac{1}{2} (\hat{\mu} + \hat{p}) \quad , \quad (39)$$

$$v^2 = \frac{1}{2} (\hat{\mu} - \hat{p}) \quad , \quad (40)$$

where

$$\hat{\mu} = (\hat{p}^2 + 4\hat{q}^2)^{1/2} \quad . \quad (41)$$

Then the final result for ξ and η , combining Eqs. (33), (34), (39) and (40), is

$$\xi = \frac{1}{2} \bar{\xi} + \left[\frac{1}{2} (\hat{\mu} + \hat{p}) \right]^{1/2} \quad , \quad (42)$$

$$\eta = \frac{1}{2} \bar{\eta} + \left[\frac{1}{2} (\hat{\mu} - \hat{p}) \right]^{1/2} \quad . \quad (43)$$

2.4 Calculation of Shearing Boundaries

The shearing boundaries, which are straightened out by the shearing transformation Eq. (9), are defined as $\bar{\eta}_U(\bar{\xi})$ and $\bar{\eta}_L(\bar{\xi})$. Thus $\bar{\eta}_U$ is the image of the upper airfoil surface and the line $\bar{\theta} = 0$ downstream of the trailing edge while $\bar{\eta}_L$ is the image of the upper half of the initial value line ($\bar{x} = -\bar{a}$) and the line $\bar{\theta} = \pi$ for $\bar{x} > -\bar{a}$.

We start by determining the image of the upper half of the airfoil in the $(\bar{\xi}, \bar{\eta})$ plane. The airfoil will be given as a set of points $(x_F, y_F)_i$ where for convenience we take the origin at the leading edge. Then the scaled airfoil coordinates in the $(\bar{x}, \bar{\theta})$ plane, for a given r , are:

$$\bar{x}_F = x_F + \ln 2 - d_s \quad , \quad (44)$$

$$\bar{\theta}_F = 4 \sin^{-1} \left(\frac{y_F}{r} \right) . \quad (45)$$

Next, the image in the (ξ, η) plane is computed from

$$\xi_F = \sinh^{-1} \left[\frac{1}{2} (\alpha - \beta) \right]^{1/2} , \quad (46)$$

$$\eta_F = \cos^{-1} \left(\frac{\bar{p}}{\cosh \xi_F} \right) , \quad (47)$$

where

$$\alpha = (\beta^2 + 4q^{-2})^{1/2} , \quad (48)$$

and \bar{p} , \bar{q} and β are given by Eqs. (19), (20) and (22). Then the image in the $(\bar{\xi}, \bar{\eta})$ plane is

$$\bar{\xi}_F = \xi_F (1 + \mu) , \quad (49)$$

$$\bar{\eta}_U = \eta_F (1 - \mu) , \quad (50)$$

and

$$\mu = \frac{\xi_0^2}{\xi_F^2 + \eta_F^2} . \quad (51)$$

The upper boundary beyond the airfoil trailing edge is the image of $\bar{\theta} = 0$ which maps to $\eta = \pi$. To calculate $\bar{\eta}_U$ in this region we first compute a uniform point distribution of $\bar{\xi}$ on the interval $(\bar{\xi}_{TE}, \bar{\xi}_{max})$. Then

corresponding values of ξ are computed by iteration from

$$\bar{\xi}(n+1) = \frac{\bar{\xi}}{1 + \mu_\pi}, \quad (52)$$

where superscript n denotes the iteration number, and

$$\mu_\pi = \frac{\xi_0^2}{\pi^2 + \xi(n)}. \quad (53)$$

We note that Eq. (52) converges quite rapidly. With a value of ξ known, $\bar{\eta}_U$ is computed from

$$\bar{\eta}_U = \pi \cdot (1 - \mu). \quad (54)$$

In the calculation of the lower $\bar{\eta}$ boundary the shearing transformation requires that the same $\bar{\xi}$ distribution be used as was determined for $\bar{\eta}_U$. The lower boundary is computed in two segments, the first on the interval $(0, \bar{\xi}_0)$, where $\bar{\xi}_0$ is the image of ξ_0 , and the second on the remaining interval $(\bar{\xi}_0, \bar{\xi}_{\max})$.

On the interval $(0, \bar{\xi}_0)$ we calculate ξ and η by iteration from the rapidly convergent formula:

$$\xi(n+1) = \frac{\bar{\xi}}{1 + \mu}, \quad (55)$$

where in this case

$$\mu = \frac{\xi_0^2}{(\xi^2 + \eta^2)(n)}, \quad (56)$$

$$\eta = \cos^{-1}(\cosh \xi(n) - 2e^{-a}). \quad (57)$$

To start the iteration we set $\mu = 1$ in Eq. (55) which from Eq. (56) is seen

to be exact at $\xi = \xi_0$. With ξ and η known, $\bar{\eta}_L$ is calculated from

$$\bar{\eta}_L = \eta \cdot (1 - \mu) . \quad (58)$$

On the interval $(\bar{\xi}_0, \bar{\xi}_{\max})$ we know from Eq. (58) that the image of $\bar{\theta} = \pi$ is

$$\bar{\eta}_L = 0 . \quad (59)$$

Thus knowing the distribution of $\bar{\eta}_U$ and $\bar{\eta}_L$ on $(0, \bar{\xi}_{\max})$ we can obtain the distribution of the shearing distance D from Eq. (11).

2.5 Stretching Functions

The approach taken here, as already mentioned, is to use one-dimensional stretching functions, as indicated by Eqs. (12), (13) and (14). In the present application the location and length scales of regions of rapid variation of the solution are known beforehand. In a $Z = \text{constant}$ plane of the computational domain, as shown in Fig. 6, clustering of $Y = \text{constant}$ lines is needed near $Y = 1$ and 0 to resolve the boundary layer developing on the airfoil and the region around the corner singularity, $\bar{x} = -\bar{a}$, $\bar{\theta} = \pi$, in the physical plane. Thus, for the variable Y a two-sided stretching function is required. Because of the primary viscous layer on the cylinder clustering is needed near $Z = 0$ which requires a one-sided stretching function for Z . The stretching function for X depends on criteria related to the flow field and the mapping geometry which will be discussed later.

Vinokur [5] has determined approximate criteria for the development of one- and two-sided stretching functions of one variable which give a uniform truncation error independent of the governing differential equation or

difference algorithm. He investigates several analytic functions but finds that only $\tan z$, where z is real or pure imaginary, satisfies all of his criteria.

We start with the stretching function for Y and note that both Y and Y_c are normalized variables as required in Vinokur's functions. In the present case, z is taken to be pure imaginary which leads to

$$Y = \frac{\tanh(Y_c \Delta\phi)}{A \sinh \Delta\phi + (1 - A \cosh \Delta\phi) \tanh(Y_c \Delta\phi)}, \tag{60}$$

where

$$A = (S_0/S_1)^{1/2}, \tag{61}$$

$$B = (S_0 S_1)^{1/2}, \tag{62}$$

and S_0 and S_1 are dimensionless slopes defined as

$$S_0 = \frac{dY_c}{dY}(0),$$

$$S_1 = \frac{dY_c}{dY}(1),$$

which control the clustering at $Y = 0$ and $Y = 1$, and $\Delta\phi$ is the solution of the following transcendental equation:

$$B = \frac{\sinh \Delta\phi}{\Delta\phi}. \tag{63}$$

To avoid solving Eq. (63) by iteration, Vinokur determines the following extremely accurate approximate solutions for small and large B :

For B < 2.7829681

$$\begin{aligned} \Delta\phi = & (6\bar{B})^{1/2} (1 - 0.15\bar{B} + 0.057321429\bar{B}^2 \\ & - 0.024907295\bar{B}^3 + 0.0077424461\bar{B}^4 \\ & - 0.0010794123\bar{B}^5) , \end{aligned} \quad (64)$$

where

$$\bar{B} = B - 1 . \quad (65)$$

For B > 2.7829681

$$\begin{aligned} \Delta\phi = & V + (1 + 1/V)\ln(2V) - 0.02041793 \\ & + 0.24902722W + 1.9496443W^2 - 2.6294547W^3 \\ & + 8.56795911W^4 , \end{aligned} \quad (66)$$

where

$$V = \ln B , \quad (67)$$

and

$$W = 1/B - 0.028527431 . \quad (68)$$

An example of this two-sided stretching function for $S_0 = 100$ and $S_1 = 10$ is shown in Fig. 7. For this case, $\Delta\phi$ computed from Eq. (66) is 5.926.

The one-sided counterpart of Eq. (6) is antisymmetric about the mid-point and, in terms of Z and Z_c , is given by

$$Z = 1 + \frac{\tanh \left[\frac{1}{2} \Delta\phi (Z_c - 1) \right]}{\tanh \frac{\Delta\phi}{2}} , \quad 0 < Z < 1 , \quad (69)$$

where $\Delta\phi$ is the solution of

$$S_0 = \frac{\sinh \Delta\phi}{\Delta\phi}, \quad (70)$$

and

$$S_0 = \frac{dz_c}{dz}(0).$$

Two examples of this one-sided stretching function, $S_0 = 10$ and 100 , are shown in Fig. 8.

The stretching function in x is required to have the following properties:

- (1) It must have the ability to cluster points near the nose of the airfoil to resolve rapid flow field variations in that region.
- (2) Control points, where grid lines are required, are the corner, $X = X_0$, and the airfoil trailing edge, $X = X_{TE}$.
- (3) Downstream of the airfoil trailing edge where flow gradients are decreasing the step size should gradually increase.
- (4) The stretching function should have continuous first derivatives.
- (5) For proper flow field resolution, the number of steps on the intervals $(0, X_0)$ and (X_0, X_{TE}) are to be parameters.

The above requirements dictate the stretching function be made up of three piecewise continuous segments on $(0, X_0)$, on (X_0, X_{TE}) and on (X_{TE}, X_{max}) .

We start by defining variables normalized on the corner location,

$$\hat{X} = \frac{X}{X_0}, \quad \hat{X}_c = \frac{X_c}{X_0}.$$

An appropriate stretching function on the first segment is given by Eq. (61) of Vinokur, viz.

$$\hat{X} = \hat{X}_c \left[1 + \frac{1}{2} (\hat{S}_0 - 1)(1 - \hat{X}_c)(2 - \hat{X}_c) \right], \quad 0 < \hat{X}_c < 1, \quad (72)$$

where \hat{S}_0 is the slope at the origin and is used to control clustering of points in that region. The uniform step size on Segment 1 is given by

$$\Delta \hat{X}_c = \frac{1.0}{N_1}, \quad (73)$$

where N_1 is the number of intervals on Segment 1. We note that $\Delta \hat{X}_c$, as given by Eq. (73), is also the step size on Segments 2 and 3.

On Segment 2, the scaled trailing edge coordinate is given by

$$(\hat{X}_c)_{TE} = 1 + N_2 \Delta \hat{X}_c, \quad (74)$$

where N_2 is the number of intervals on Segment 2. We note that $(\hat{X}_c)_{TE} \neq \hat{X}_{TE}$.

The constraints to be satisfied by the stretching function of Segment 2 are:

$$\left. \begin{aligned} \hat{X} = 1, \quad \hat{X}' = \hat{X}'_1 \quad \text{on} \quad \hat{X}_c = 1 \\ \hat{X} = \hat{X}_{TE} \quad \text{on} \quad \hat{X}_c = (\hat{X}_c)_{TE} \end{aligned} \right\}, \quad (75)$$

where

$$\hat{X}'_1 = \left. \frac{d\hat{X}}{d\hat{X}_c} \right|_{\hat{X}_c=1}$$

which from Eq. (72) is

$$\hat{X}'_1 = \frac{1}{2}(3 - \hat{S}_0). \quad (73)$$

With three constraints a parabola is appropriate. The resulting stretching function is

$$\hat{X} = 1 + [\hat{X}'_1 + A(\hat{X}_c - 1)](\hat{X}_c - 1), \quad (77)$$

where

$$A = \frac{\hat{X}_{TE} - 1 - \hat{X}'_1[(\hat{X}_c)_{TE} - 1]}{[(\hat{X}_c)_{TE} - 1]^2}. \quad (78)$$

On Segment 3 a geometric progression is used to increase the step size in \hat{X} . Requiring continuity of \hat{X} at the junction with Segment 2, we have

$$\hat{X}_k = \hat{X}_{TE} + \Delta\hat{X}_1 \left(\frac{1 - \hat{C}^{k-1}}{1 - \hat{C}} \right), \quad k > 2, \quad (79)$$

where \hat{C} is the constant step size ratio defined by,

$$\hat{C} = \frac{\Delta\hat{X}_k}{\Delta\hat{X}_{k-1}} > 1.$$

Continuity of the first derivative at the junction is ensured by choosing $\Delta\hat{X}_1$ equal to the last $\Delta\hat{X}$ on Segment 2. No attempt is made to match \hat{X}_{\max} exactly.

The stretching function for \hat{X} is seen to have four parameters, \hat{S}_0 , N_1 , N_2 and \hat{C} , which provide considerable flexibility in the point distribution of \hat{X} . A typical example is shown in Fig. 9.

3. RESULTS AND DISCUSSION3.1 Generation of the Grid

The step-by-step procedure to generate a grid in the physical plane for a given airfoil shape and initial value plane location is as follows:

- (1) The uniform computational grid $(X_{c_i}, Y_{c_j}, Z_{c_k})$ is first established and then (X_i, Y_j, Z_k) are calculated via the stretching functions described in Section 2.5.
- (2) With (X_i, Y_j, Z_k) known, \bar{r}_k is determined from

$$\bar{r}_k = Z_k \cdot \quad (80)$$

Then for \bar{r} fixed, the points in the (X, Y) plane are transformed to the $(\bar{\xi}, \bar{\eta})$ plane by

$$\bar{\xi}_{ijk} = X_i \cdot \quad (81)$$

$$\bar{\eta}_{ijk} = Y_j D_{ik} + (\bar{\eta}_L)_{ik} \cdot \quad (82)$$

where

$$D_{ik} = (\bar{\eta}_U)_{ik} - (\bar{\eta}_L)_{ik} \cdot \quad (83)$$

By Eq. (45), $\bar{\theta}_F$ depends on r and hence \bar{r} and therefore $\bar{\eta}_L$ and $\bar{\eta}_U$ must be computed anew for each value of \bar{r} . The procedure used here is to calculate more points than needed on the shearing boundaries for a given \bar{r} and then to use Lagrange cubic interpolation to determine $\bar{\eta}_L$ and $\bar{\eta}_U$ for a given $\bar{\xi}$.

(3) With $(\bar{\xi}, \bar{\eta})$ known, the transformation to the (ξ, η) plane is

$$\xi_{ijk} = \frac{1}{2} \bar{\xi}_{ijk} + \left[\frac{1}{2} (\hat{\mu} + \hat{p}) \right]_{ijk}^{1/2}, \quad (84)$$

$$\eta_{ijk} = \frac{1}{2} \bar{\eta}_{ijk} + \left[\frac{1}{2} (\hat{\mu} - \hat{p}) \right]_{ijk}^{1/2}, \quad (85)$$

where

$$\hat{\mu} = (\hat{p}^2 + 4\hat{q}^2)^{1/2}, \quad (86)$$

$$\hat{p} = \frac{1}{4} (\bar{\xi}^2 - \bar{\eta}^2) - \xi_0^2, \quad (87)$$

$$\hat{q} = \frac{1}{4} \bar{\xi} \bar{\eta}. \quad (88)$$

(4) Next, the points in the (ξ, η) plane are transformed to the $(\bar{x}, \bar{\theta})$ plane by

$$\bar{x}_{ijk} = \ln(\cosh \xi_{ijk} - \cos \eta_{ijk}), \quad (89)$$

$$\bar{\theta}_{ijk} = \cos^{-1} \left(\frac{1 - \cosh \xi_{ijk} \cos \eta_{ijk}}{\cosh \xi_{ijk} - \cos \eta_{ijk}} \right). \quad (90)$$

(5) The final step is to compute the cylindrical coordinates of each grid point from:

$$x_{ijk} = \bar{x}_{ijk} + d_s - \ln 2, \quad (91)$$

$$\theta_{ijk} = \frac{1}{4} \bar{\theta}_{ijk}, \quad (92)$$

$$r_k = R_c + (R_t - R_c) \bar{r}_k. \quad (93)$$

3.2 Features of the Grid

The shearing transformation applied at the fourth stage necessarily produces a nonorthogonal grid in the $(\bar{x}, \bar{\theta})$ plane. The nonorthogonality is smallest on the lower shearing boundary, under most conditions, and largest at the airfoil surface on the upper shearing boundary, as can be seen from Fig. 5. On the upper (airfoil) boundary the nonorthogonality near the leading edge ($\bar{\xi} = 0$) can be controlled by proper location of the singularity of the unwrapping transformation, Eq. (6). Away from the leading edge the only control over nonorthogonality is to keep the airfoil reasonably thin, say eight percent or less, which will maintain $\bar{\eta}_U$ as close to the image of $\eta = \pi$ as possible.

The parameter which controls grid orthogonality near the airfoil leading edge is d_s in Eq. (3). The most nearly orthogonal system in this region is produced when the leading edge maps into an $\eta = \text{constant}$ line. In the (x, θ) plane such a line is closely approximated by a parabola centered about $\theta = 0$ and is effectively characterized by its radius of curvature at the origin, given by

$$\rho_o = \frac{1}{\left. \frac{d^2x}{d\theta^2} \right|_{\theta=0}} \quad . \quad (94)$$

We determine ρ_o by setting $\eta = \eta_{LE} = \text{constant}$ in Eqs. (15) and (16), differentiating the result twice with respect to θ to find $d^2\bar{x}/d\bar{\theta}^2$, plus noting that $d\bar{x}/d\bar{\theta} = 0$ at $\theta = 0$ and by virtue of Eqs. (3) and (5) that

$$\frac{d^2x}{d\theta^2} = 16 \frac{d^2\bar{x}}{d\bar{\theta}^2} \quad .$$

The result is

$$\rho_o = -\frac{1}{16} \frac{\sin^2 \eta_{LE}}{\cos \eta_{LE}} e^{-\bar{x}_{LE}} \quad (95)$$

From Eq. (3) evaluated at the airfoil leading edge ($x = 0$) we have

$$\bar{x}_{LE} = \ln 2 - d_s \quad (96)$$

and from Eq. (17) with $\xi = 0$ and $\eta = \eta_{LE}$ we find that

$$\cos \eta_{LE} = 1 - 2e^{-d_s} \quad (97)$$

from which it follows that

$$\sin \eta_{LE} = 2[e^{-d_s}(1 - e^{-d_s})]^{1/2} \quad (98)$$

Hence, Eq. (95) for ρ_o becomes

$$\rho_o = \frac{1}{8} \left(\frac{1 - e^{-d_s}}{2e^{-d_s} - 1} \right) \quad (99)$$

which can be solved for d_s to yield,

$$d_s = \ln \left(\frac{1 + 16 \rho_o}{1 + 8 \rho_o} \right) \quad (100)$$

Next, we fit the airfoil leading edge by an osculating parabola, viz.

$$x = K\theta^2 \quad (101)$$

where $K = x_i/\theta_i^2$ and (x_i, θ_i) are appropriate airfoil coordinates near the leading edge. The radius of curvature of the airfoil at the leading edge is, from Eq. (101),

$$\rho_{LE} = \frac{1}{x_o''} = \frac{\theta_i^2}{2x_i} \quad (102)$$

The optimum value of d_s (which produces the most nearly orthogonal grid near $\bar{\xi} = 0$) is obtained by equating ρ_{LE} and ρ_o . Thus, d_s can then be determined from Eq. (100). Figure 10 shows the variation of $\bar{\eta}_U$ with $\bar{\xi}$ for a six percent thick Joukowski airfoil for three values of d_s , one of which was determined by Eqs. (100) and (102). In these three cases, we have $d_s \ll d_L$ which has the effect of limiting the influence of d_s on $\bar{\eta}_U$ to the region $0 < \bar{\xi} < \bar{\xi}_0$ where here $\bar{\xi}_0 \cong 0.87$. As r increases from R_c to R_L the leading edge radius of curvature of the airfoil decreases because θ_P decreases--see Eq. (45). Thus d_s must be decreased accordingly.

On the lower shearing boundary the nonorthogonality arises from the mapping of the initial value line (IVL) by Eq. (7). In the (ξ, η) plane the IVL is very nearly half of an ellipse with the ratio of the semi-major to semi-minor axes lengths, defined as $\lambda = \eta_o/\xi_o$ (η_o is the value of η on the IVL at $\xi = 0$) given by

$$\lambda = \frac{\cos^{-1}(1 - 2e^{-a})}{\cosh^{-1}(1 + 2e^{-a})} . \tag{103}$$

Figure 11, in which λ is plotted versus "a", shows that as "a" becomes large λ approaches unity and therefore the IVL approaches a semi-circle in the (ξ, η) plane. Thus for $\bar{\eta}_L$ to have the smallest maximum (at $\bar{\xi} = 0$) and hence for $\bar{\xi} = \text{constant}$ lines at $\bar{\eta} = \bar{\eta}_L$ to be as nearly orthogonal as possible, "a" should be large, say 3 or 4, a circumstance desirable on physical grounds anyway.

At the image of the airfoil trailing edge in the $(\bar{\xi}, \bar{\eta})$ plane (Points D and E in Fig. 5) when the trailing edge angle is finite the derivative of $\bar{\eta}_U$ with respect to $\bar{\xi}$ will be discontinuous. At the ends of the IVL (Points A and C in Fig. 5) the behavior of $\bar{\eta}_L$ is cusp-like which means that the second derivative of $\bar{\eta}_L$ with respect to $\bar{\xi}$ is discontinuous. These discontinuities produce similar type discontinuities in $Y = \text{constant}$ lines via the shearing transformation. This behavior is one of the disadvantages of algebraic mappings involving shearing transformation which is absent in grids generated by solving elliptic partial differential equations. The discontinuous behavior of derivatives of $Y = \text{constant}$ lines in the physical plane should therefore be accounted for in the calculation of affected metric coefficients and in the numerical method of solution of the viscous flow equations.

3.3 Numerical Examples

For simplicity a symmetric Joukowski airfoil was used in the numerical examples of the grid. The ordinates of this airfoil (for unit chord) are given by,

$$y_F = \frac{4\tau}{3\sqrt{3}} (1 - x_F)[4 x_F(1 - x_F)]^{1/2} , \tag{104}$$

where x_F is measured from the airfoil leading edge and τ is the maximum thickness to chord ratio. Two example grids in the $(\bar{x}, \bar{\theta})$ plane are presented with parameters listed in Table 1 below. The parameter J is the number of points in the Y direction.

Parameter	Case 1	Case 2
N_1	---	15
N_2	---	15
J	31	31
d_{IVL}	3.0	3.0
d_s	0.05	0.05
d_{OB}	3.0	3.0
τ	0.12	0.06
R_c	1.0	1.0
r/R_c	1.0	1.0
S_0	10	10
S_1	10	10
\hat{S}_0	---	0.2
\hat{C}	---	1.2

Table 1. Grid parameters for Numerical Examples

Case 1 is shown in Fig. 12 and Case 2 in Fig. 13. Case 1 has no stretching function in X and no $X = \text{constant}$ line through the corner. The non-orthogonality of the grid in Case 1 (12% thick) is seen to be more pronounced at the airfoil surface than in Case 2 (6% thick) which bears out the remark made earlier. Notice that both examples are for the grid in the $(\bar{x}, \bar{\theta})$ plane on the cylinder surface ($r = R_c$) which corresponds to the intersection of the fin with the cylinder. Hence in these examples, by Eq. (45), the airfoil thickness in terms of $\bar{\theta}$ is a maximum and thus the nonorthogonality is most pronounced.

The computer code listing is given in the appendix.

References

- (1) Jameson, A., "Iterative Solution of Transonic Flows over Airfoils and Wings, Including Flow at Mach 1," *Comm. Pure Appl. Math.* 27, 283-309 (1974).
- (2) Caughey, D. A. and A. Jameson, "Numerical Calculation of Transonic Potential Flow about Wing-Body Combinations," *AIAA Jour.* 17, 175-181 (1979).
- (3) Caughey, D. A. and A. Jameson, "Progress in Finite-Volume Calculations for Wing-Fuselage Combinations," *AIAA Jour.* 18, 1281-1288 (1980).
- (4) Caughey, D. A., "A Systematic Procedure for Generating Useful Conformal Mappings," *Int. Jour. Numer. Meth. Engin.* 12, 1651-1657 (1978).
- (5) Vinokur, M., "On One-Dimensional Stretching Functions for Finite-Difference Calculations," NASA CR-3313 (October 1980).

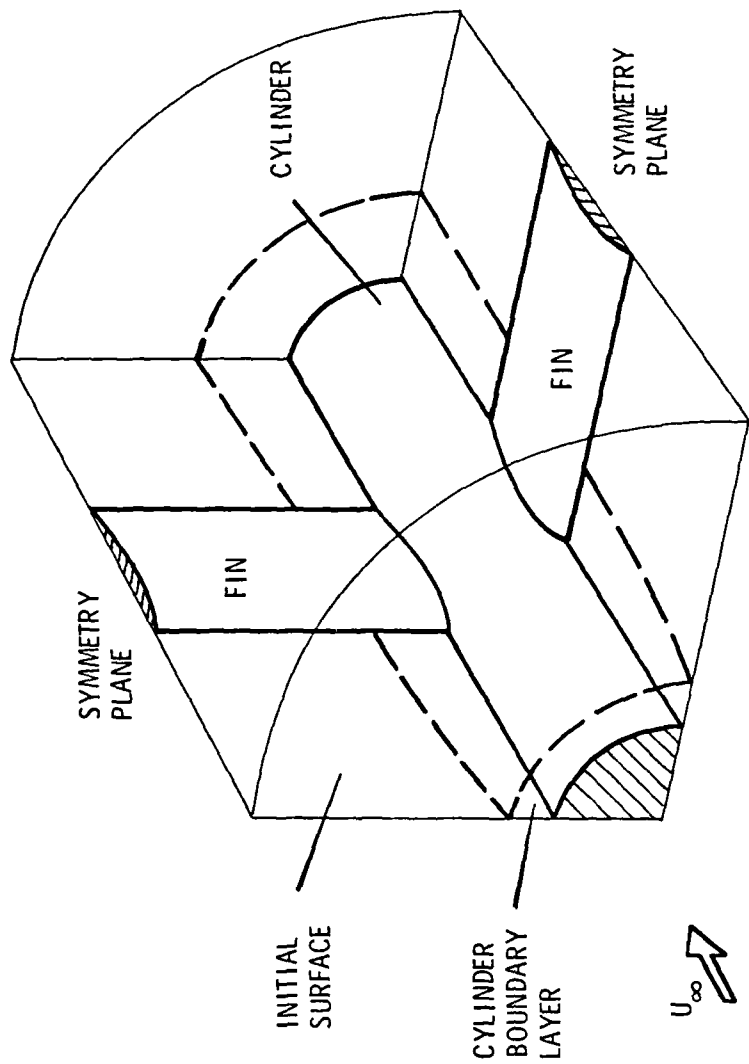


Figure 1. Schematic of Geometry and Computational Domain.

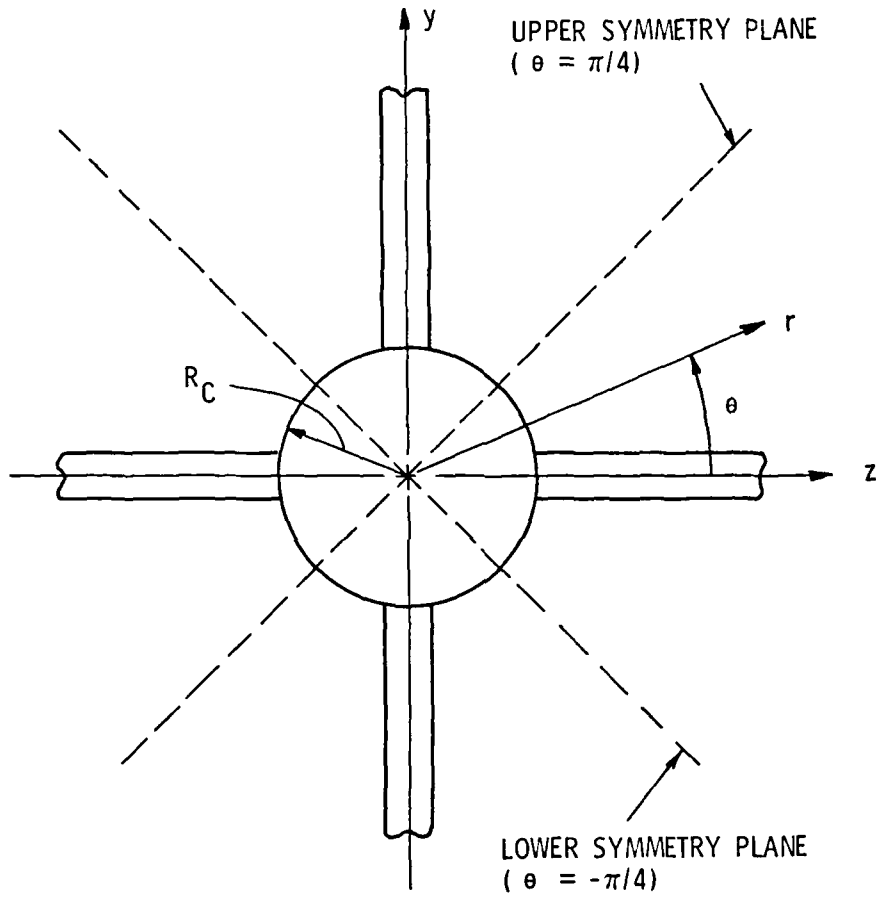


Figure 2. Coordinate System in Crossflow Plane.

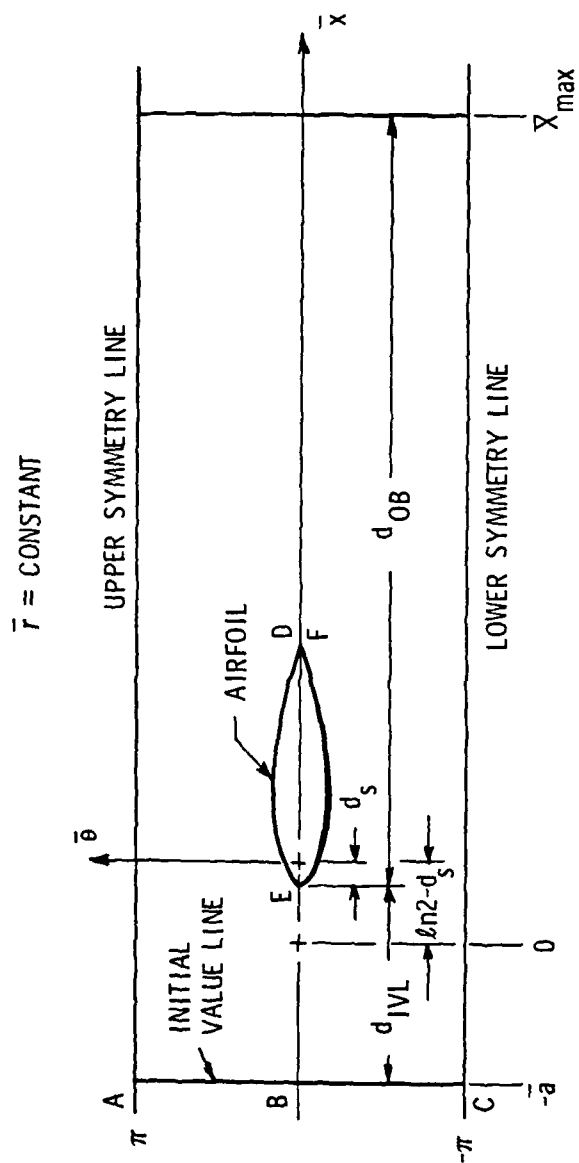


Figure 3. Computational Domain in $(\bar{x}, \bar{\theta})$ Plane.

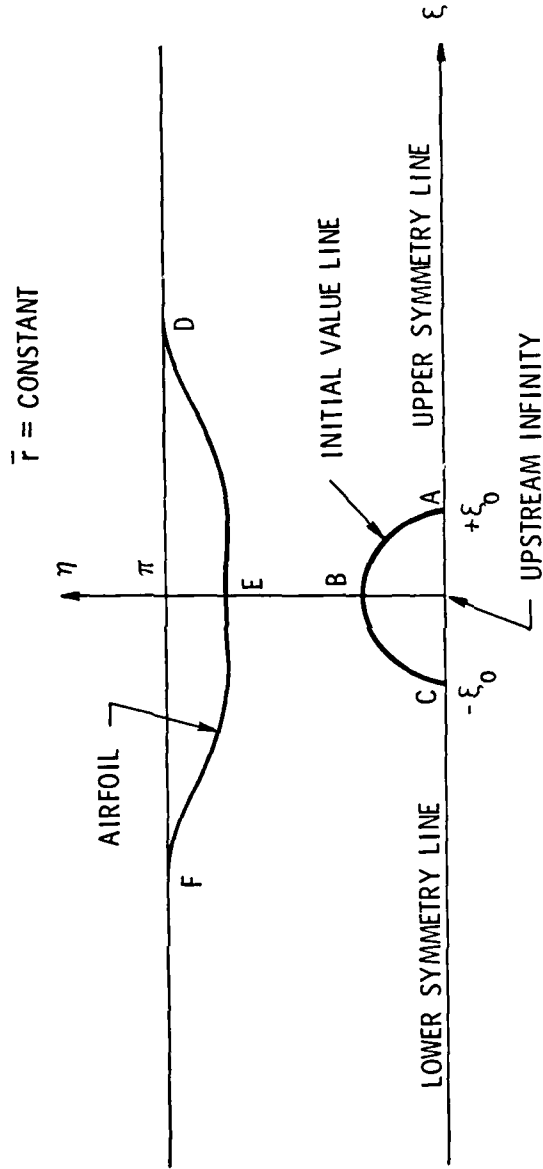


Figure 4. Boundary Images in (ξ, η) Plane.

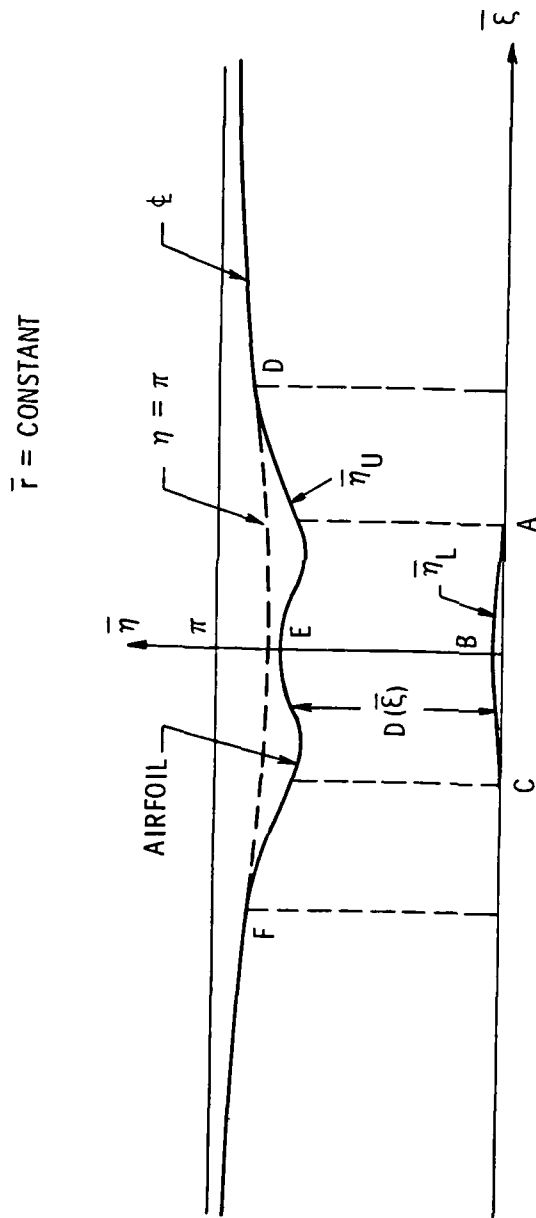


Figure 5. Boundary Images in $(\bar{\xi}, \bar{\eta})$ Plane.

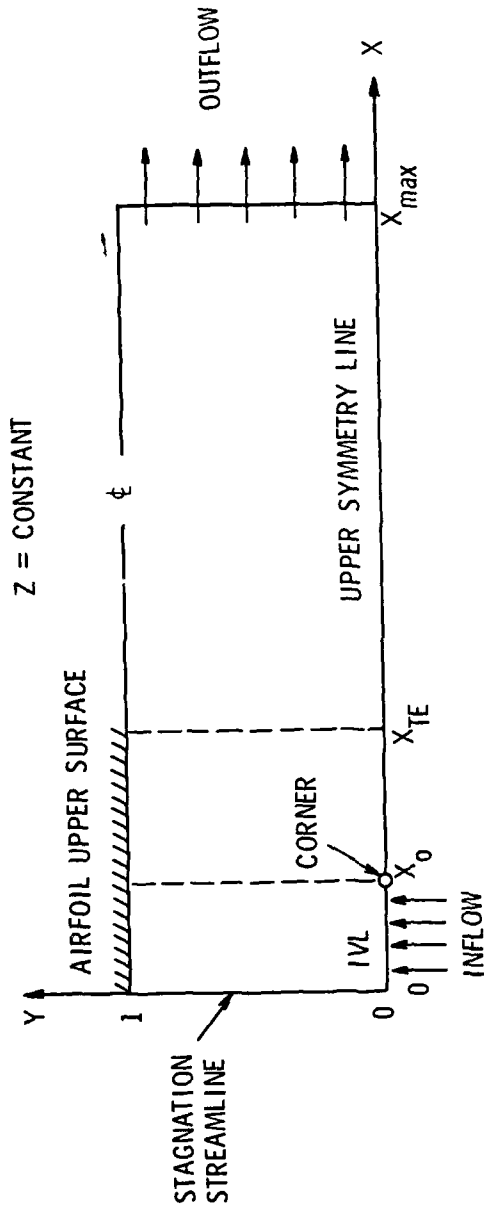


Figure 6. Schematic of Computational Plane.

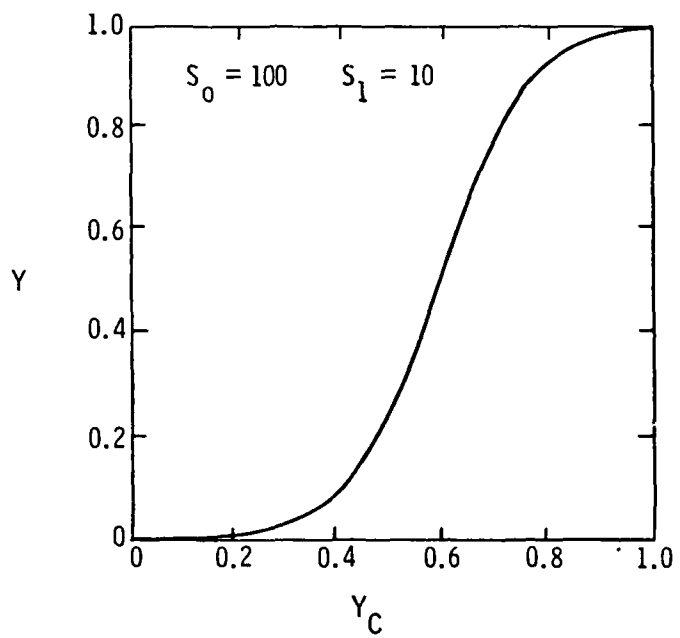


Figure 7. Two-Sided Stretching Function for Y.

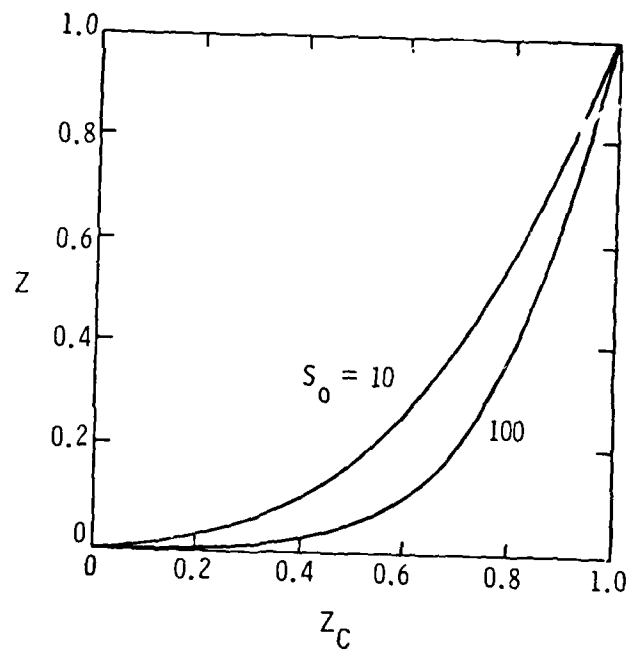


Figure 8. One-Sided Stretching Function for Z.

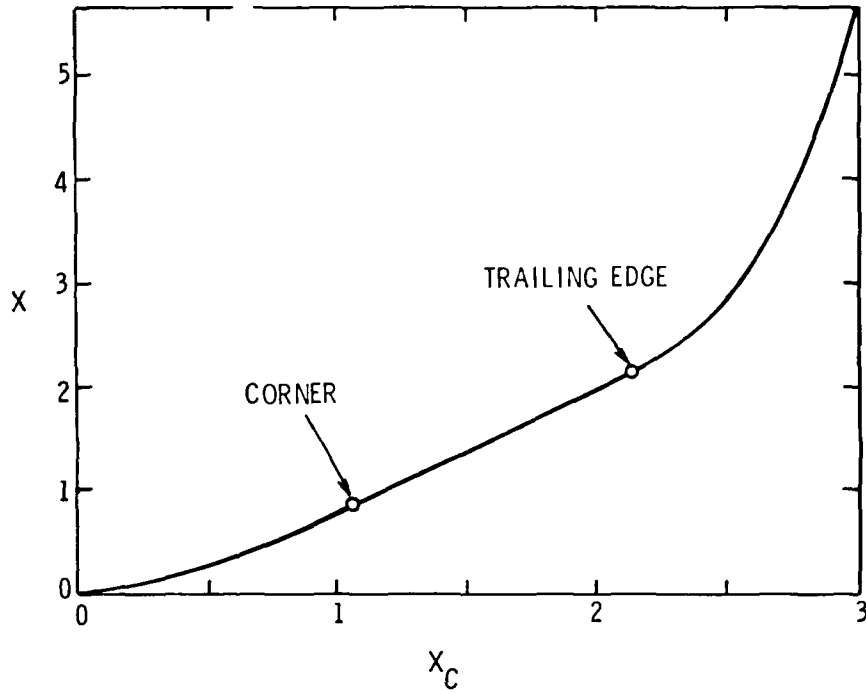


Figure 9. Three Segment Stretching Function for X.

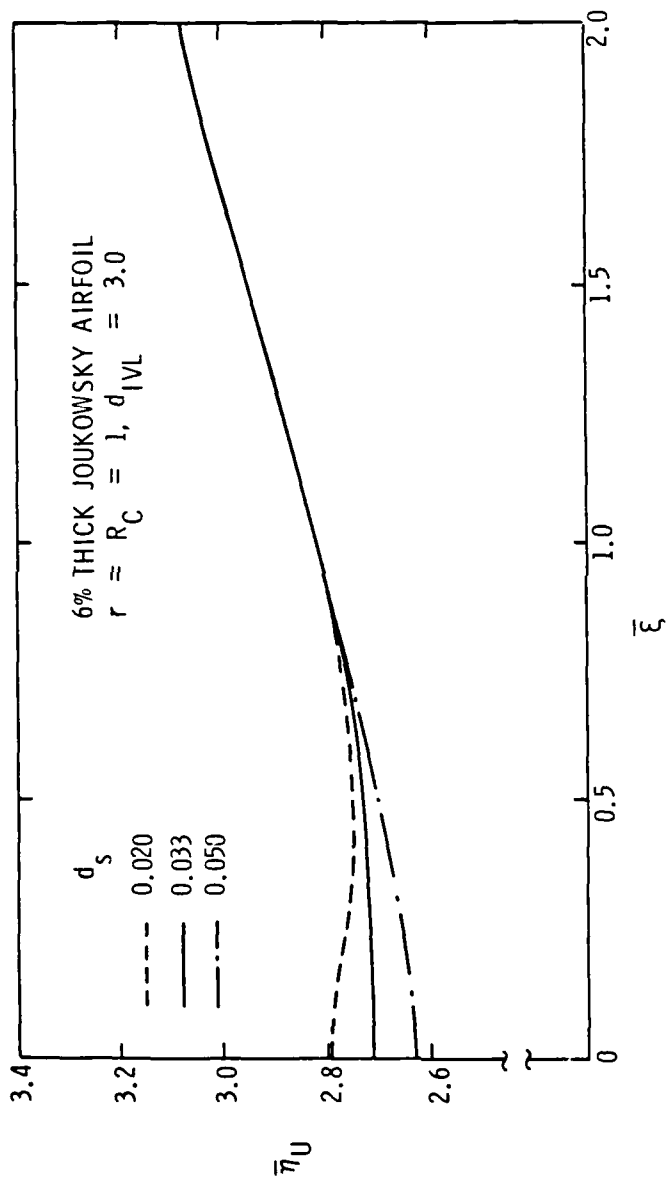


Figure 10. Effect of Singularity location on Upper Shearing Boundary.

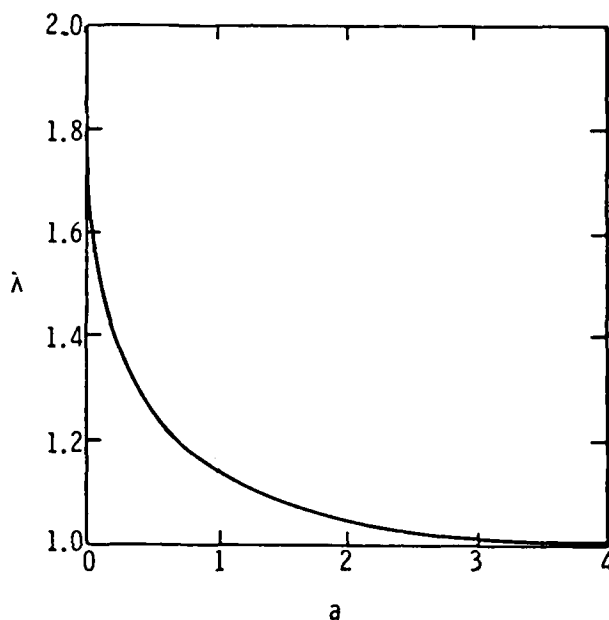


Figure 11. Ellipticity of Initial Value Line in (ξ, η) Plane.

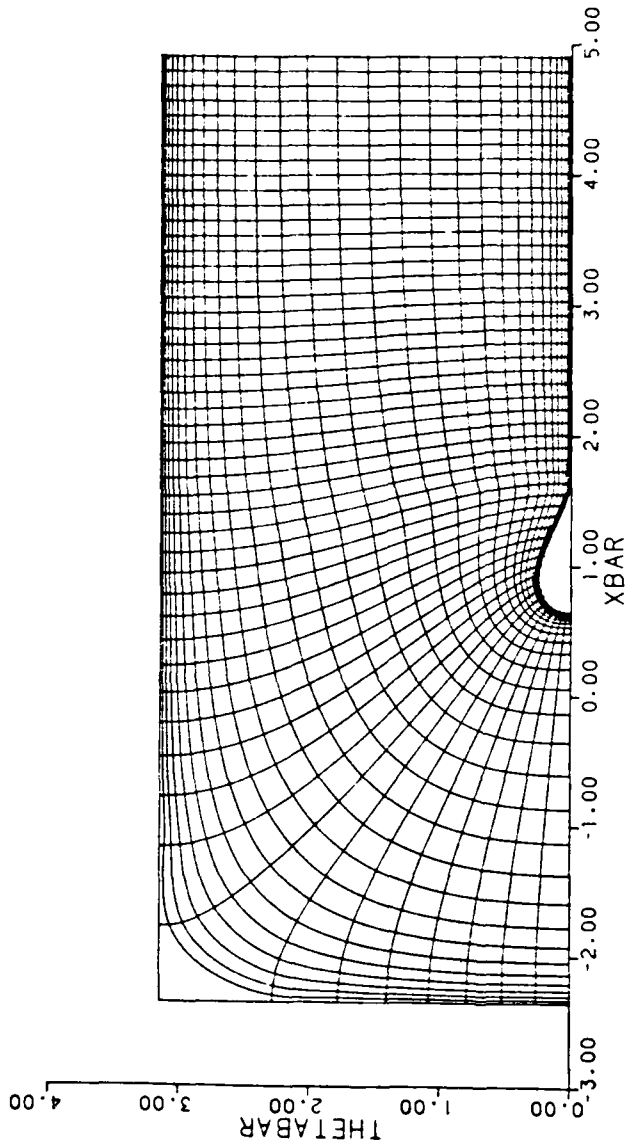


Figure 12. Grid for a Twelve Percent Thick Joukowski Airfoil.

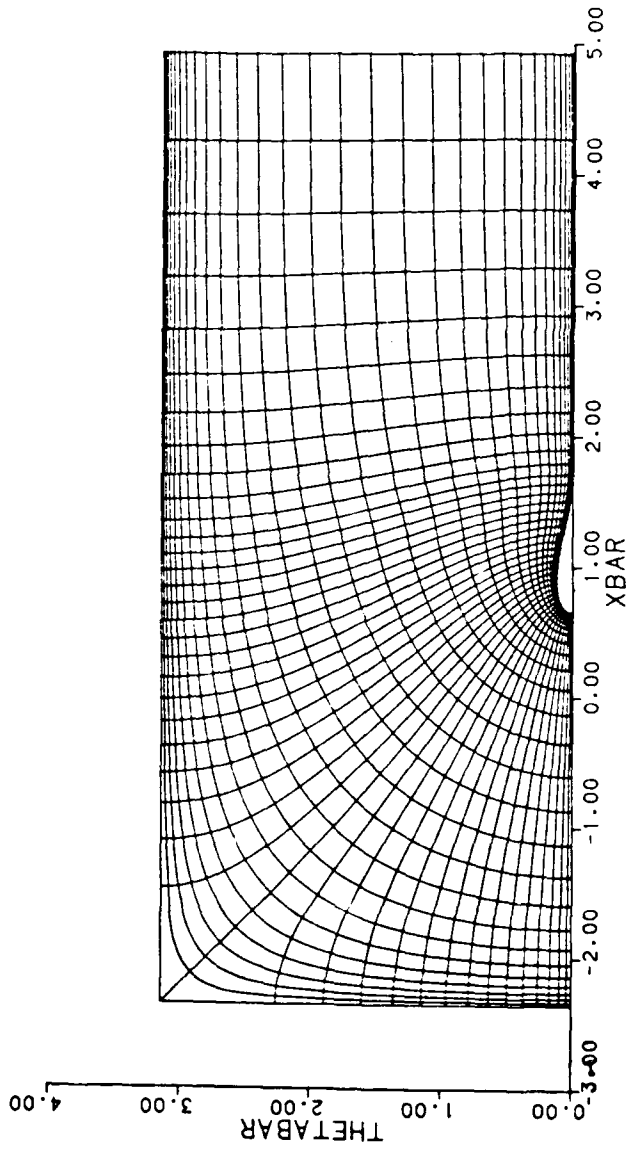


Figure 13. Grid for a Six Percent Thick Joukowski Airfoil.

Appendix: Grid Generation Computer Code Listing


```

10 C PROGRAM NAME: CGRID3
20 C THIS PROGRAM COMPUTES A SURFACE FITTED C-GRID FOR A FIN
30 C CYLINDER BODY.
40 C THE FIN IN THIS VERSION IS A SYMMETRIC JOUKOWSKY AIRFOIL.
50 C THIS IS THE 3-D VERSION.
60 C*****
70 C IMPLICIT REAL*8 (A-H,O-Z)
80 C COMMON /BLK01/ IMAX,JMAX,ITE,ITEM,ILAST,ISEG1,ISEG2
90 C COMMON /BLK02/ XIEM,XIO,XIBO
100 C COMMON /BLK03/ C1,C2,C3,C4,C5,PI,PISQ
110 C COMMON /BLK04/ XF(101),YF(101)
120 C COMMON /BLK05/ XIB(151),SBAR(151),ETABL(151)
130 C COMMON /BLK06/ SY0,SY1,SZ0,SX0,SSR
140 C COMMON /BLK07/ ZC(151),BIGZ(151)
150 C
160 C 1 FORMAT(5I4)
170 C 2 FORMAT(5F10.4)
180 C 10 FORMAT(1H1,4X,'INPUT PARAMETERS FOR C-GRID')
190 C 11 FORMAT(1H0,9X,'ISEG1 =',I6/10X,'ISEG2 =',I6/10X,'JMAX =',
200 C 1I6/10X,'KMAX =',I6/10X,'ITE =',I6)
210 C 12 FORMAT(10X,'DIVL =',F10.4/10X,'DOB =',F10.4/
220 C 110X,'TAU =',F10.4/10X,'RC =',F10.4/10X,'RT =',F10.4/10X,
230 C 2'SY0 =',F10.4/10X,'SY1 =',F10.4/10X,'SZ0 =',F10.4/10X,'SX0 =',
240 C 3F10.4/10X,'SSR =',F10.4)
250 C 13 FORMAT(1H0)
260 C 14 FORMAT(5X,'STACKED C-GRID FOR FIN-CYLINDER GEOMETRY')
270 C 15 FORMAT(10X,'DS =',D14.4)
280 C
290 C INPUT REQUIREMENTS
300 C
310 C ISEG1 = NO. INTERVALS ON FIRST X-SEGMENT.
320 C ISEG2 = NO. INTERVALS ON SECOND X-SEGMENT.
330 C IMAX = NO. POINTS IN X-DIRECTION.
340 C JMAX = NO. POINTS IN Y-DIRECTION.
350 C KMAX = NO. POINTS IN Z-DIRECTION.
360 C ITE = NO. POINTS ON AIRFOIL INITIALLY.
370 C DIVL = DISTANCE FROM AIRFOIL L.E. TO INITIAL VALUE LINE.
380 C DS = DISTANCE FROM AIRFOIL L.E. TO SINGULARITY OF
390 C COORDINATE SYSTEM.
400 C DOB = DISTANCE FROM AIRFOIL I.E. TO OUTFLOW BOUNDARY.
410 C TAU = AIRFOIL MAX. THICKNESS TO CHORD RATIO.
420 C RC = INNER CYLINDER RADIUS, IN TERMS OF AIRFOIL CHORD.
430 C RT = OUTER CYLINDER RADIUS, IN TERMS OF AIRFOIL CHORD.
440 C SY0 = Y-STRETCHING PARAMETER AT AIRFOIL SURFACE.
450 C SY1 = Y-STRETCHING PARAMETER AT INITIAL SURFACE.
460 C SZ0 = Z-STRETCHING PARAMETER AT INNER CYLINDER.
470 C SX0 = INITIAL X-STRETCHING PARAMETER, SEGMENT 1.
480 C SSR = X-GEOMETRIC PROGRESSION RATIO, SEGMENT 3.
490 C
500 C READ(5,1) ISEG1,ISEG2,JMAX,KMAX,ITE
510 C READ(5,2) DIVL,DOB
520 C READ(5,2) TAU,RC,RT
530 C READ(5,2) SY0,SY1,SZ0,SX0,SSR
540 C ITEM=ITE-1
550 C WRITE(6,10)
560 C WRITE(6,11) ISEG1,ISEG2,JMAX,KMAX,ITE
570 C WRITE(6,12) DIVL,DOB,TAU,RC,RT,SY0,SY1,SZ0,SX0,SSR
580 C WRITE(6,13)
590 C WRITE(6,14)
600 C
610 C C3=2.0D0*TAU/DSQRT(27.0D0)

```

```

620      PI=3.14159265358979D0
630      PISQ=PI*PI
640      XE=1.0D0+D08
650      C
660      C      CALCULATE AIRFOIL COORDINATES.
670      C
680      CALL FOIL
690      C
700      C      CALCULATE ZC AND BIGZ.
710      C
720      CALL STRFZ(ZC,BIGZ,KMAX,SZ0)
730      DELR=RT-RC
740      C
750      C      BEGIN CALCULATION OF STACKED GRID.
760      C
770      DO 50 K=1,KMAX
780      RAD=RC+DELR*BIGZ(K)
790      C
800      C      CALCULATE DS - DISTANCE FROM AIRFOIL LEADING EDGE TO
810      C      SINGULARITY OF UNWRAPPING TRANSFORMATION.
820      C
830      THF=DASIN(YF(4)/RAD)
840      RHO=0.5D0*THF*THF/XF(4)
850      DS=DLOG((1.0D0+16.0D0*RHO)/(1.0D0+8.0D0*RHO))
860      WRITE(6,13)
870      WRITE(6,15) DS
880      WRITE(6,13)
890      C1=DEXP(-(DIVL+DS))
900      C2=2.0D0*C1
910      RHS=DSQRT(4.0D0*C1*(1.0D0+C1))
920      CALL ASINH(XI0,RHS)
930      C4=DLOG(2.0D0)-DS
940      C5=XI0*XI0
950      XIB0=2.0D0*XI0
960      C
970      C      CALCULATE XIBM - COORDINATE OF DOWNSTREAM BOUNDARY IN XI BAR -
980      C      ETA BAR PLANE.
990      C
1000     XBE=XE+C4
1010     TERM=DEXP(XBE)-1.0D0
1020     RHS=DSQRT(TERM*TERM-1.0D0)
1030     CALL ASINH(XIE,RHS)
1040     XIBM=XIE*(1.0D0+C5/(PISQ+XIE*XIE))
1050     C
1060     CALL SHEAR(RAD)
1070     KK=K
1080     CALL XTGRID(KK,RAD)
1090     50 CONTINUE
1100     STOP
1110     END
1120     SUBROUTINE SHEAR(RAD)
1130     C*****
1140     C      THIS SUBROUTINE CALCULATES SHAR VS. XI BAR, TO BE USED IN THE
1150     C      SHEARING TRANSFORMATION.
1160     C*****
1170     IMPLICIT REAL*8 (A-H,O-Z)
1180     COMMON /BLK01/ IMAX,JMAX,ITE,ITEM,ILAST,ISEG1,ISEG2
1190     COMMON /BLK02/ XIBM,XI0,XIB0
1200     COMMON /BLK03/ C1,C2,C3,C4,C5,PI,PISQ
1210     COMMON /BLK04/ XF(101),YF(101)
1220     COMMON /BLK05/ XIB(151),SBAR(151),ETABL(151)

```

```

1230 C
1240 DIMENSION ETABU(151)
1250 C
1260 10 FORMAT(5X,'SHEARING BOUNDARY IN XIBAR - ETABAR PLANE')
1270 11 FORMAT(1H0)
1280 12 FORMAT(5X,'I',6X,'XIBAR',9X,'ETABL',9X,'ETABU',9X,'SBAR')
1290 13 FORMAT(16,4D14.4)
1300 14 FORMAT(1H0,4X,'UNABLE TO CONVERGE XI IN 50 ITERATIONS'/5X,
1310 1'XIBAR =',D14.4)
1320 C
1330 C COMPUTE NORMALIZED AIRFOIL COORDINATES FOR GIVEN CYLINDRICAL
1340 C RADIUS AND TRANSFORM TO XI BAR - ETA BAR PLANE. THIS STEP
1350 C GIVES THE FIRST PORTION OF THE UPPER BOUNDARY.
1360 C
1370 WRITE(6,11)
1380 WRITE(6,10)
1390 WRITE(6,11)
1400 T1=RAD*RAD
1410 DO 50 I=1,ITE
1420 YF1=YF(I)
1430 THF=DASIN(YF1/RAD)
1440 XBF1=XF(I)+C4
1450 THBFI=4.000*THF
1460 C
1470 T2=DEXP(XBF1)
1480 PBAR=1.000-T2*DCOS(THBFI)
1490 QBAR=T2*DSIN(THBFI)
1500 QSQ=QBAR*QBAR
1510 BETA=1.000-PBAR*PBAR-QSQ
1520 ALPHA=DSQRT(BETA*BETA+4.000*QSQ)
1530 RHS=DSQRT(0.500*(ALPHA-BETA))
1540 CALL ASINH(XIF,RHS)
1550 ARG=PBAR/DCOSH(XIF)
1560 IF((ARG+1.000).LT.0.000) ARG=-1.000
1570 ETAF=DACOS(ARG)
1580 C
1590 XMU=C5/(XIF*XIF+ETAF*ETAF)
1600 XIB(I)=XIF*(1.000+XMU)
1610 ETABU(I)=ETAF*(1.000-XMU)
1620 50 CONTINUE
1630 C
1640 C CONTINUE UPPER BOUNDARY CALCULATION BEYOND AIRFOIL T.E.
1650 C TO XIBM.
1660 C
1670 DXIB=0.200
1680 ILAST=ITE+(XIBM-XIB(ITE))/DXIB
1690 IF(ILAST.GT.151) ILAST=151
1700 ITEP=ITE+1
1710 WRITE(6,12)
1720 DO 100 I=ITEP,ILAST
1730 XIBAR=XIB(I-1)+DXIB
1740 XIB(I)=XIBAR
1750 XIL=XIBAR
1760 DO 70 IT=1,50
1770 XMU=C5/(PISQ+XIL*XIL)
1780 XI=XIBAR/(1.000+XMU)
1790 IF(DABS(XI-XIL).LT.1.0D-08) GO TO 80
1800 70 XIL=XI
1810 WRITE(6,14) XIBAR
1820 STOP
1830 80 ETABU(I)=PI*(1.000-XMU)

```

```

1840      100 CONTINUE
1850      C
1860      C      CALCULATE LOWER BOUNDARY IN XI BAR - ETA BAR PLANE AND
1870      C      SBAR.
1880      C
1890      DO 200 I=1,ILAST
1900      XIBAR=XIB(I)
1910      IF(XIBAR.GE.XIB0) GO TO 140
1920      XIL=XIBAR
1930      XMU=1.000
1940      DO 120 IT=1,50
1950      XI=XIBAR/(1.000+XMU)
1960      ARG=DCOSH(XI)-C2
1970      ETA=DACOS(ARG)
1980      XMU=C5/(XI*XI+ETA*ETA)
1990      IF(DABS(XI-XIL).LT.1.00-08) GO TO 130
2000      120 XIL=XI
2010      WRITE(6,14) XIBAR
2020      STOP
2030      130 ETABL(I)=ETA*(1.000-XMU)
2040      GO TO 150
2050      140 ETABL(I)=0.000
2060      150 SBAR(I)=ETABU(I)-ETABL(I)
2070      *RITE(6,13) I,XIB(I),ETABL(I),ETABU(I),SBAR(I)
2080      200 CONTINUE
2090      RETURN
2100      END
2110      SUBROUTINE XTGRID(K,RAD)
2120      C*****
2130      C      THIS SUBROUTINE CALCULATES THE GRID IN THE XBAR - THETABAR
2140      C      PLANE.
2150      C*****
2160      IMPLICIT REAL*8 (A-H,O-Z)
2170      COMMON /BLK01/ IMAX,JMAX,ITE,ITEM,ILAST,ISEG1,ISEG2
2180      COMMON /BLK02/ XIBM,XIO,XIB0
2190      COMMON /BLK03/ C1,C2,C3,C4,C5,PI,PISQ
2200      COMMON /BLK05/ XIB(151),SBAR(151),ETABL(151)
2210      COMMON /BLK06/ SY0,SY1,SZ0,SX0,SSR
2220      COMMON /BLK07/ ZC(151),BIGZ(151)
2230      C
2240      DIMENSION BIGX(151),BIGY(151)
2250      DIMENSION XC(151),YC(151)
2260      C
2270      11 FORMAT(1H0)
2280      12 FORMAT(5X,'I',5X,'J',5X,'K',6X,'XC',12X,'YC',12X,'ZC',12X,
2290      1'R',13X,'X',13X,'THETA')
2300      13 FORMAT(3I6,6D14.4)
2310      C
2320      C      SET UP GRID IN COMPUTATIONAL PLANE.
2330      C
2340      XBTE=XIB(ITE)
2350      NPTE=ISEG1+ISEG2+1
2360      CALL STRFX(XC,BIGX,ISEG1,ISEG2,IMAX,SX0,SSR,XIB0,XBTE,XIBM)
2370      CALL STRFY(YC,BIGY,JMAX,SY0,SY1)
2380      C
2390      C      DETERMINE GRID IN PHYSICAL PLANE.
2400      C
2410      I=1
2420      XIBAR=0.000
2430      SBI=SBAR(1)
2440      ETBLI=ETABL(1)

```

```

2450      WRITE(6,11)
2460      WRITE(6,12)
2470      WRITE(6,11)
2480      DO 70 J=1,JMAX
2490      ETABAR=ETHLI+SBI*BIGY(J)
2500      P=0.2500*ETABAR*ETABAR+C5
2510      XI=0.000
2520      ETA=0.500*ETABAR+DSQRT(P)
2530      XBAR=DLOG(1.000-DCOS(ETA))
2540      THBAR=0.000
2550      XX=XBAR-C4
2560      THETA=0.000
2570      WRITE(6,13) I,J,K,XC(I),YC(J),ZC(K),RAD,XX,THETA
2580 70 CONTINUE
2590      IBEG=1
2600      IEND=ITE
2610      DO 100 I=2,IMAX
2620      XIBAR=BIGX(I)
2630      IF(I.LE.NPTE) GO TO 80
2640      IBEG=ITE
2650      IEND=ILAST
2660  C
2670  C      INTERPOLATE TO FIND SBAR AND ETABL CORRESPONDING TO XIBAR.
2680  C
2690 80 CALL INTERP(XIB,SBAR,XIBAR,SBI,IBEG,IEND,INT,0)
2700 CALL INTERP(XIB,ETABL,XIBAR,ETBLI,IBEG,IEND,INT,1)
2710  C
2720      WRITE(6,11)
2730      WRITE(6,12)
2740      WRITE(6,11)
2750      DO 100 J=1,JMAX
2760      ETABAR=ETBLI+SBI*BIGY(J)
2770      Q=0.2500*XIBAR*ETABAR
2780      P=0.2500*(XIBAR*XIBAR-ETABAR*ETABAR)-C5
2790      XMU=DSQRT(P*P+4.000*Q*Q)
2800      XI=0.500*XIBAR+DSQRT(0.500*(XMU+P))
2810      ETA=0.500*ETABAR+DSQRT(0.500*(XMU-P))
2820  C
2830      T1=DCOSH(XI)
2840      T2=DCOS(ETA)
2850      ARG1=T1-T2
2860      XBAR=DLOG(ARG1)
2870      THBAR=DACUS((1.000-T1*T2)/ARG1)
2880      THETA=0.2500*THBAR
2890      XX=XBAR-C4
2900      WRITE(6,13) I,J,K,XC(I),YC(J),ZC(K),RAD,XX,THETA
2910 100 CONTINUE
2920      RETURN
2930      END
2940      SUBROUTINE ASINH(ARG,RHS)
2950  C*****
2960  C      THIS SUBROUTINE COMPUTES THE INVERSE HYPERBOLIC SINE USING
2970  C      NEWTON'S METHOD.
2980  C*****
2990      IMPLICIT REAL*8 (A-H,O-Z)
3000  C
3010      10 FORMAT(1H0,4X,'INVERSE HYPERBOLIC SINE CALCULATION FAILED FOR
3020      1SINH(X) =',D14.7)
3030  C
3040      TEST=DABS(RHS)
3050      IF(TEST.GT.1.000) GO TO 30

```

```

3060     ARG=RHS
3070     GO TO 40
3080     30 ARG=DLOG(2.0D0*TEST)*DSIGN(1.0D0,RHS)
3090     40 CONTINUE
3100     DO 50 K=1,50
3110     FA=DSINH(ARG)-RHS
3120     FPA=DCOSH(ARG)
3130     DARG=-FA/FPA
3140     IF(DABS(DARG).LT.1.0D-10) RETURN
3150     ARG=ARG+DARG
3160     50 CONTINUE
3170     WRITE(6,10) RHS
3180     RETURN
3190     END
3200     SUBROUTINE FOIL
3210     C*****
3220     C   THIS SUBROUTINE GENERATES (X,Y) COORDINATES FOR A SYMMETRIC
3230     C   JOUKOWSKY AIRFOIL.
3240     C*****
3250     IMPLICIT REAL*8 (A-H,O-Z)
3260     COMMON /BLK01/ IMAX,JMAX,ITE,ITEM,ILAST,ISEG1,ISEG2
3270     COMMON /BLK03/ C1,C2,C3,C4,C5,PI,PISQ
3280     COMMON /BLK04/ XF(101),YF(101)
3290     C
3300     10 FORMAT(5X,'AIRFOIL COORDINATES')
3310     11 FORMAT(1H0)
3320     12 FORMAT(5X,'I',6X,'XF',13X,'YF')
3330     13 FORMAT(I6,2D14.4)
3340     C
3350     DTH=PI/ITEM
3360     XF(1)=0.0D0
3370     YF(1)=0.0D0
3380     DO 50 I=2,ITEM
3390     C   TH=(I-1)*DTH
3400     C   T1=DCOS(TH)
3410     XF(I)=0.5D0*(1.0D0-T1)
3420     YF(I)=C3*(1.0D0+T1)*DSIN(TH)
3430     50 CONTINUE
3440     XF(ITE)=1.0D0
3450     YF(ITE)=0.0D0
3460     WRITE(6,11)
3470     WRITE(6,10)
3480     WRITE(6,11)
3490     *RITE(6,12)
3500     DO 60 I=1,ITE
3510     60 WRITE(6,13) I,XF(I),YF(I)
3520     RETURN
3530     END
3540     SUBROUTINE INTERP(XX,YY,XINT,YINT,IBEG,IEND,INT,ISW)
3550     C*****
3560     C   THIS SUBROUTINE USES LAGRANGE CUBIC INTERPOLATION TO
3570     C   DETERMINE YINT FOR A GIVEN XINT.
3580     C
3590     C   XX   = INDEPENDENT VARIABLE.
3600     C   YY   = DEPENDENT VARIABLE.
3610     C   IBEG = INITIAL INDEX FOR INTERPOLATION RANGE.
3620     C   IEND = FINAL INDEX FOR INTERPOLATION RANGE.
3630     C   INT  = UPPER INDEX OF INTERPOLATION INTERVAL.
3640     C   ISW  = INTERPOLATION INTERVAL SEARCH SWITCH.
3650     C           0 PERFORM SEARCH.
3660     C           1 OMIT SEARCH.

```

```

3670 C*****
3680     IMPLICIT REAL*8 (A-H,O-Z)
3690 C
3700     DIMENSION XX(151),YY(151)
3710 C
3720     IF(ISW.GT.0) GO TO 75
3730 60 DO 70 I=IBEG,IEND
3740     INT=I
3750     IF(XX(I).GT.XINT) GO TO 75
3760 70 CONTINUE
3770 75 IF(INT.EQ.(IBEG+1)) GO TO 80
3780     IF(INT.EQ.IEND) GO TO 90
3790     I1=INT-2
3800     I2=INT-1
3810     I3=INT
3820     I4=INT+1
3830     GO TO 100
3840 90 I1=IBEG
3850     I2=IBEG+1
3860     I3=IBEG+2
3870     I4=IBEG+3
3880     GO TO 100
3890 90 I1=IEND-3
3900     I2=IEND-2
3910     I3=IEND-1
3920     I4=IEND
3930 100 CONTINUE
3940     X1=XX(I1)
3950     X2=XX(I2)
3960     X3=XX(I3)
3970     X4=XX(I4)
3980     CF1=(XINT-X2)*(XINT-X3)*(XINT-X4)/((X1-X2)*(X1-X3)*(X1-X4))
3990     CF2=(XINT-X1)*(XINT-X3)*(XINT-X4)/((X2-X1)*(X2-X3)*(X2-X4))
4000     CF3=(XINT-X1)*(XINT-X2)*(XINT-X4)/((X3-X1)*(X3-X2)*(X3-X4))
4010     CF4=(XINT-X1)*(XINT-X2)*(XINT-X3)/((X4-X1)*(X4-X2)*(X4-X3))
4020     YINT=CF1*YY(I1)+CF2*YY(I2)+CF3*YY(I3)+CF4*YY(I4)
4030     RETURN
4040     END
4050     SUBROUTINE STRFY(XI,T,NPT,SY0,SY1)
4060 C*****
4070 C     THIS SUBROUTINE GENERATES A NONUNIFORM POINT DISTRIBUTION
4080 C     USING VINOKURS TWO-SIDED STRETCHING FUNCTION, AS GIVEN IN
4090 C     NASA CR-3133.
4100 C*****
4110     IMPLICIT REAL*8 (A-H,O-Z)
4120 C
4130     DIMENSION XI(151),T(151)
4140 C
4150 C     COMPUTE XI.
4160 C
4170     DXI=1.000/(NPT-1)
4180     DO 40 J=1,NPT
4190 40 XI(J)=(J-1)*DXI
4200 C
4210 C     COMPUTE DELTA Y.
4220 C
4230     A=DSQRT(SY0/SY1)
4240     B=DSQRT(SY0*SY1)
4250     TEST=2.782968100
4260     IF(B.GT.TEST) GO TO 50
4270     YBAR=B-1.000

```

```

4280      DELY=((( (-0.0010794123D0*YBAR+0.0077424461D0)*YBAR
4290      1-0.024907295D0)*YBAR+0.057321429D0)*YBAR-0.15D0)*YBAR
4300      2+1.0D0)*DSQRT(6.0D0*YBAR)
4310      GO TO 60
4320      50 V=DLOG(B)
4330      W=1.0D0/B-0.028527431D0
4340      DELY=((( (8.56795911D0**W-2.6294547D0)*W+1.9496443D0)*W
4350      1+0.24902722D0)*W-0.02041793D0+V+(1.0D0+1.0D0/V)*
4360      2DLOG(2.0D0*V)
4370      60 CONTINUE
4380      C
4390      C      COMPUTE T.
4400      C
4410      C1=A*DSINH(DELY)
4420      C2=1.0D0-A*DCOSH(DELY)
4430      DO 70 I=1,NPT
4440      T(I)=DTANH(DELY*XI(I))
4450      T(I)=FN/(C1+C2*FN)
4460      70 CONTINUE
4470      RETURN
4480      END
4490      SUBROUTINE STRFX(XI,T,NSEG1,NSEG2,NMAX,SX0,SSR,XIBO,XBTE,XIBM)
4500      C*****
4510      C      THIS SUBROUTINE GENERATES A NONUNIFORM POINT DISTRIBUTION
4520      C      SPECIALIZED TO THE COORDINATE WRAPPED AROUND THE AIRFOIL.
4530      C*****
4540      IMPLICIT REAL*8 (A-H,O-Z)
4550      C
4560      DIMENSION XI(151),T(151)
4570      C
4580      C      SEGMENT NUMBER 1.
4590      C
4600      TTE=XBTE/XIBO
4610      TMAX=XIBM/XIBO
4620      DXI=1.0D0/NSEG1
4630      NP1=NSEG1+1
4640      S1=0.5D0*(SX0-1.0D0)
4650      DO 50 I=1,NP1
4660      XX=(I-1)*DXI
4670      XI(I)=XX
4680      50 T(I)=XX*(1.0D0+S1*(1.0D0-XX))*(2.0D0-XX)
4690      C
4700      C      SEGMENT NUMBER 2.
4710      C
4720      AA=0.5D0*(3.0D0-SX0)
4730      XWTE=NSEG2*DXI
4740      BB=(TTE-1.0D0-AA*XWTE)/(XWTE*XWTE)
4750      NP2=NSEG2+1
4760      DO 60 K=2,NP2
4770      I=NSEG1+K
4780      XW=(K-1)*DXI
4790      XI(I)=1.0D0+XW
4800      60 T(I)=1.0D0+XW*(AA+XW*BB)
4810      C
4820      C      SEGMENT NUMBER 3.
4830      C
4840      N3=NSEG1+NSEG2
4850      NP3=N3+1
4860      XITE=XI(NP3)
4870      DT1=T(NP3)-T(N3)
4880      S1=DT1/(SSR-1.0D0)

```



```

4890      KMAX=151-NP3
4900      DO 70 K=2,KMAX
4910      I=N3+K
4920      XI(I)=XITE+(K-1)*DXI
4930      TI=TTE+S1*(SSP**(K-1)-1.000)
4940      T(I)=TI
4950      IF(TI.GE.TMAX) GO TO 80
4960      70 CONTINUE
4970      80 NMAX=I
4980      C
4990      C      RESCALE VARIABLES.
5000      C
5010      SCALE=XITE/XITE
5020      DO 90 I=1,NMAX
5030      XI(I)=SCALE*XI(I)
5040      90 T(I)=XIB0*T(I)
5050      RETURN
5060      END
5070      SUBROUTINE STRFZ(XI,T,NPT,S0)
5080      C*****
5090      C      THIS SUBROUTINE GENERATES A NONUNIFORM POINT DISTRIBUTION USING
5100      C      VINOKURS ONE-SIDED STRETCHING FUNCTION.
5110      C*****
5120      IMPLICIT REAL*8 (A-H,O-Z)
5130      C
5140      DIMENSION XI(151),T(151)
5150      C
5160      C      COMPUTE XI.
5170      C
5180      DXI=1.000/(NPT-1)
5190      DO 40 K=1,NPT
5200      40 XI(K)=(K-1)*DXI
5210      C
5220      C      COMPUTE DELTA Y.
5230      C
5240      TEST=2.7829681D0
5250      IF(S0.GT.TEST) GO TO 50
5260      YBAR=S0-1.000
5270      DELY=(((((-0.0010794123D0*YBAR+0.0077424461D0)*YBAR
5280      1-0.024907295D0)*YBAR+0.057321429D0)*YBAR-0.15D0)*YBAR
5290      2+1.000)*DSQRT(6.000*YBAR)
5300      GO TO 60
5310      50 V=DLOG(S0)
5320      W=1.000/S0-0.028527431D0
5330      DELY=(((8.56795911D0*W-2.6294547D0)*W+1.9496443D0)*W
5340      1+0.24902722D0)*W-0.02041793D0+V+(1.000+1.000/V)*
5350      2DLOG(2.000*V)
5360      60 CONTINUE
5370      C
5380      C      COMPUTE T.
5390      C
5400      C1=0.5D0*DELY
5410      C2=1.0D0/DTANH(C1)
5420      DO 70 K=1,NPT
5430      T(K)=1.0D0+C2*DTANH(C1*(XI(K)-1.0D0))
5440      70 CONTINUE
5450      RETURN
5460      END

```

DISTRIBUTION LIST FOR UNCLASSIFIED TM 83-45
by G. H. Hoffman, dated 30 March 1983

Office of Naval Research
Department of the Navy
800 North Quincy Street
Arlington, VA 22217
Attn: R. E. Whitehead
(Copy No. 1)

Naval Research Laboratory
Department of the Navy
Washington, DC 20390
Attn: Library
(Copy No. 13)

Office of Naval Research
Department of the Navy
800 North Quincy Street
Arlington, VA 22217
Attn: C. Lee
(Copy No. 2)

Superintendent
Code 1424
Naval Post Graduate School
Monterey, CA 93949
(Copy No. 14)

Commander
Naval Sea Systems Command
Department of the Navy
Washington, DC 20362
Attn: T. E. Peirce
Code NSEA-63R31
(Copy No. 3)

NASA Lewis Research Center
21000 Brookpark Road
Cleveland, OH 44135
Attn: P. M. Sockol
Code MS 77-5
(Copy No. 15)

Commander
Naval Underwater Systems Center
Department of the Navy
Newport, RI 02840
Attn: D. J. Goodrich
Code 3634
(Copy No. 4)

Professor C. L. Merkle
Department of Mechanical Engineering
The Pennsylvania State University
University Park, PA 16802
(Copy No. 16)

Commander
David W. Taylor Naval Ship R&D Center
Department of the Navy
Bethesda, MD 20084
Attn: Library
(Copy No. 5)

Director
Applied Research Laboratory
The Pennsylvania State University
Post Office Box 30
State College, PA 16801
Attn: R. E. Henderson
(Copy No. 17)

Commander
Naval Surface Weapons Center
Department of the Navy
Silver Spring, MD 20910
Attn: Library
(Copy No. 6)

Director
Applied Research Laboratory
The Pennsylvania State University
Post Office Box 30
State College, PA 16801
Attn: B. R. Parkin
(Copy No. 18)

Defense Technical Information Center
5010 Duke Street
Cameron Station
Alexandria, VA 22314
(Copies 7 through 12)

Director
Applied Research Laboratory
The Pennsylvania State University
Post Office Box 30
State College, PA 16801
Attn: S. A. Abdallah
(Copy No. 19)

Director
Applied Research Laboratory
The Pennsylvania State University
Post Office Box 30
State College, PA 16801
Attn: M. W. McBride
(Copy No. 20)

Director
Applied Research Laboratory
The Pennsylvania State University
Post Office Box 30
State College, PA 16801
Attn: G. C. Lauchle
(Copy No. 21)

Director
Applied Research Laboratory
The Pennsylvania State University
Post Office Box 30
State College, PA 16801
Attn: W. S. Gearhart
(Copy No. 22)

Director
Applied Research Laboratory
The Pennsylvania State University
Post Office Box 30
State College, PA 16801
Attn: K. C. Kaufman
(Copy No. 23)

Director
Applied Research Laboratory
The Pennsylvania State University
Post Office Box 30
State College, PA 16801
Attn: G. H. Hoffman
(Copy No. 24)

Director
Applied Research Laboratory
The Pennsylvania state University
Post Office Box 30
State College, PA 16801
Attn: J. J. Eisenhuth
(Copy No. 25)

Director
Applied Research Laboratory
The Pennsylvania State University
Post Office Box 30
State College, PA 16801
Attn: Garfield Thomas Water Tunnel Files
(Copy No. 26)

VE
MED
8